ISIJ International, Vol. 54 (2014), No. 4, pp. 801–809

Water-gas Shift Reaction in an Olivine Pellet Layer in the Upper Part of Blast Furnace Shaft

Antti KEMPPAINEN,[1)*] Tuomas ALATARVAS,[1)] Mikko ILJANA,[1)] Juho HAAPAKANGAS,[1)] Olli MATTILA,[2)] Timo PAANANEN[2)] and Timo FABRITIUS[1)]

1) Laboratory of Process Metallurgy, University of Oulu, P.O Box 4300 FI-90014 Finland.
2) Ruukki Metals Oy, Rautaruukintie 155, Raahe, FI-92100 Finland.

(*Received on September 12, 2013; accepted on November 19, 2013*)

In order to reduce CO_2 emissions in the iron and steel industry, the utilization of H_2 gas as a reducing agent is a feasible option. The use of hydrogen bearing injectants in the lower blast furnace (BF) area increases H_2O concentration in the upper part of the BF shaft and the charging of moist burden has a similar effect as well. For efficient BF operation, it is important to investigate the effect of high H_2 and therefore high H_2O concentrations in the reducing gas. This study focuses on the upper BF shaft area where hematite to magnetite reduction takes place and temperature is in the range of the forward water-gas shift reaction (WGSR). The effect of the WGSR on the composition of the reducing gas was estimated by experimental methods. A layer furnace (LF) was used to determine the temperature for the occurrence of the WGSR under simulated BF shaft conditions. The feed gas conversion was investigated in an olivine pellet layer. The WGSR was observed in an empty LF with CO–H_2O–N_2 gas at 500°C. With CO–CO_2–H_2O–N_2 gas the WGSR was observed in an olivine pellet layer at 400–450°C and in a pre-reduced magnetite pellet layer at 300–400°C indicating the catalyzing effect of magnetite on the WGSR. The results offer additional information about the effect of high H_2O concentration on the composition of the reducing gas through the WGSR. The occurrence of the WGSR in the actual BF and its effects were discussed.

KEY WORDS: water-gas shift reaction; iron oxide; magnetite; reduction; hydrogen; water vapor; carbon monoxide; carbon dioxide.

1. Introduction

Partial replacement of carbonaceous reductants by hydrogen bearing injectants in the blast furnace (BF) process is an effective way to reduce CO_2 emissions. This leads to an increase in H_2 and H_2O concentrations in the BF shaft and several studies[1–3)] have investigated the reduction behavior of iron oxides when H_2 or H_2–H_2O is added to the reducing gas. However, other authors[2,4,5)] have noticed that a remarkable increase of H_2O concentration in the BF shaft caused by the H_2 addition in the lower BF area also has other effects in the BF shaft. One is the water-gas shift reaction (WGSR), which becomes more significant with an increasing H_2O concentration in the reducing gas. The WGSR, presented in Eq. (1), is a reversible, equilibrium controlled exothermic chemical reaction, usually assisted by a catalyst, and is the reaction of water vapor with carbon monoxide to produce carbon dioxide and hydrogen gas. Since there is no change in the volume from reactants to products, the reaction is not affected by pressure.[6–10)] Calculated $\Delta G = 0$ for the WGSR via HSC Chemistry software is approximately at 810°C and at higher temperatures the reaction towards the reactants is favorable.[11)]

$$CO(g) + H_2O(g) \leftrightarrow H_2(g) + CO_2(g), \quad \Delta H^0_{298K} = -41.09\ kJ/mol \quad \text{..... (1)}$$

This research work focuses on the upper BF shaft area where hematite to magnetite reduction takes place and the temperature is in the range of the forward WGSR. Since magnetite is known to catalyze the WGSR,[6–10)] this may have an effect on the composition of the reducing gas and therefore affect the reduction reactions in the upper BF shaft area and utilization of the BF top gas. Thus, it is important to investigate the effect of high H_2O concentration on the reducing gas in the upper BF shaft area.

In this study the conditions of the BF shaft were simulated with a laboratory scale layer furnace and the occurrence of the forward WGSR was determined in an olivine pellet layer, a phenomenon which needs to be studied further.

2. Experimental

2.1. Experimental Device

The layer furnace (LF) originally presented by Alatarvas *et al.*[12)] was used for experimental investigation and is shown in **Fig. 1**. An arbitrary atmosphere profile can be set to the LF consisting of N_2, CO, CO_2, H_2 and H_2O gas com-

* Corresponding author: E-mail: antti.kemppainen@oulu.fi
DOI: http://dx.doi.org/10.2355/isijinternational.54.801

ponents. The gas composition and temperature profile can either be changed manually or with a preset program dependent on time. The furnace tube, having a diameter of 80 mm, can be loaded with a 1.0 m high bed of desired materials and heated up to 1 200°C. The temperature of the feed gas is measured with a thermocouple located in the center of the tube between the pre-heating block and the furnace tube. Therefore, the temperature of the feed gas can be adjusted to the same temperature as the lowest part of the furnace, preventing low-temperature gas entering the tube and cooling the lowest part of the furnace. The material bed is heated by three separately controlled resistors, in order to accurately control the furnace temperature in the vertical direction. The furnace element resistors are controlled by the temperature values acquired by three separate thermocouples at the heights of 15 cm, 48 cm and 81 cm, positioned in the center of the furnace tube in the horizontal direction. The temperature data of all four sections are automatically stored on the computer. The furnace is equipped with six gas sampling points (GSP). The lowest GSP, labeled as 1, is located between the pre-heating block and the furnace tube below the material bed. The gas analysis of the first GSP represents the feed gas composition and acts as a reference point for the other gas analyses. GSPs labeled as 2–6 are positioned in the material bed in the center of the furnace tube at the heights of 5, 10, 15, 48 and 81 cm, respectively, measured from the bottom of the tube. The gas is sampled via six electromagnetic valves, of which only one is open at a time. The valves are computer-controlled and the GSPs are automatically changed in ascending order of 1 to 6. Any of the sampling points can be bypassed. The sample is conveyed by a vacuum pump through a water bath to the dew point (DP) meter, which determines the water vapor concentration. After that the gas is led to the freezer where the water vapor is condensed with a copper tube equipped with flow deflectors. Next, the temperature of gas is leveled in a water bath and further led to the gas analyzer (Portable Infrared Coal gas Analyzer Gasboard-3100P, produced by Wuhan Cubic Optoelectronics Co., Ltd.), measuring the concentration of CO, CO_2, H_2, CH_4 and O_2 gas components. Gas concentration values are automatically stored on the computer in desired time intervals. Finally, the sampling gas is led to the exhaustion flue. In order to prevent water vapor condensation, the gas feed line is heated up to approximately 90°C. Moreover, the lines between the layer furnace gas sampling tubes and the freezer are heated up to approximately 60°C.

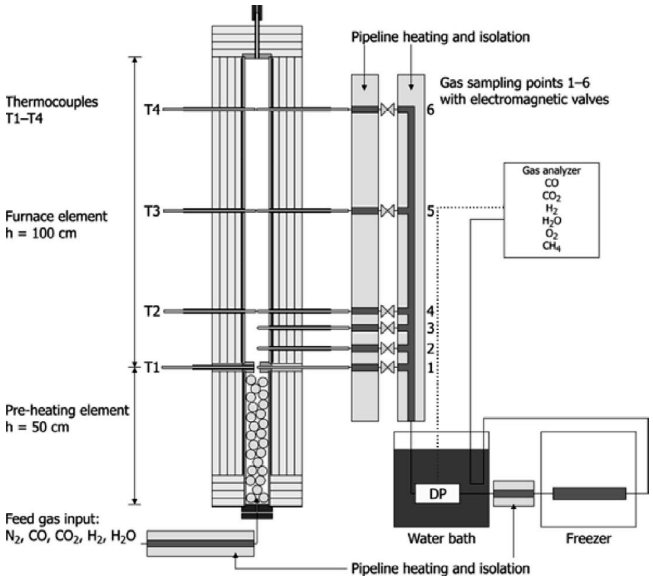

Fig. 1. Schematic layout of the layer furnace with auxiliary instruments.

2.2. Materials and Conditions

Hematite pellets with low magnetite content fluxed with olivine were used in the LF experiments. The chemical composition of the pellets is shown in **Table 1**. Void fraction of the packed pellet bed was measured by a water displacement method and was estimated to be 0.45 in the LF tube. Three LF experiments were carried out: 1) in an empty LF, 2) in a LF filled with olivine pellets (hematite) and 3) in a LF filled with olivine pellets pre-reduced to magnetite. The conditions in the experiments are shown in **Table 2**, labeled as ELF, HPL and MPL, respectively. The LF was heated at 3°C/min rate in each experiment which was sufficiently slow heating rate to maintain in the LF with the packed pellet bed. The LF heating rate with packed pellet bed in HPL experiment is shown in **Fig. 2**. T1–T4 in Fig. 2 represent the four thermocouples shown in Fig. 1. The reactions in the furnace tube were observed by analyzing the gas samples taken from the gas sampling points 1–4 shown in Fig. 1. This study focuses on GSPs 1–4 to clarify the presentation of the results since it was noticed that GSPs 5 and 6 gave no relevant information. During the experiments each of the six electromagnetic valves were kept open for 2 minutes at a time when a gas sample was obtained and then automatically changed to the next sample in an ascending order of 1 to 6. The gas analysis data was sent to a computer and stored

Table 1. Chemical composition of the low-magnetite olivine pellets.

Component	Content (mass-%)
Fe_{tot}	67.1
FeO	0.1
CaO	0.38
SiO_2	1.69
MgO	1.25
Al_2O_3	0.30

Table 2. Conditions in the LF experiments.

Experiment	ELF	HPL	MPL
H_2 (%)	0	0	0
H_2O (%)	8	8	8
CO (%)	42	17	17
CO_2 (%)	–	25	25
N_2 (%)	50	50	50
Gas flow rate (l/min)	15	15	15
Heating rate (°C/min)	3	3	3
Max temperature (°C)	700	500	500
Height of the packed bed (m)	–	1.0	1.0
Timeheld at max temp. (min)	–	150	150

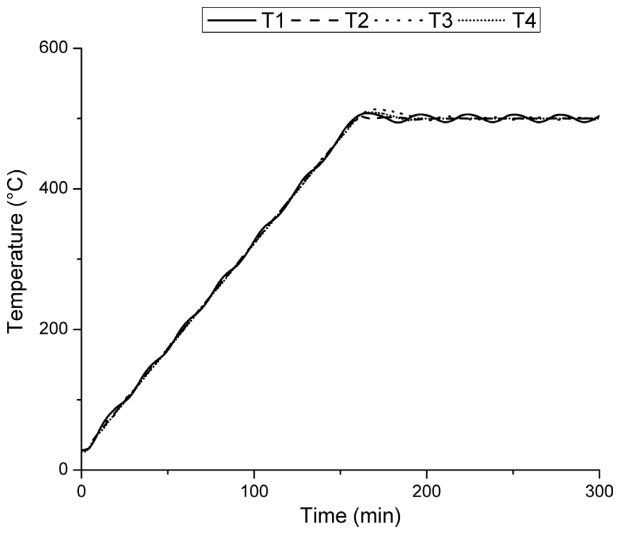

Fig. 2. LF heating rate in the HPL experiment.

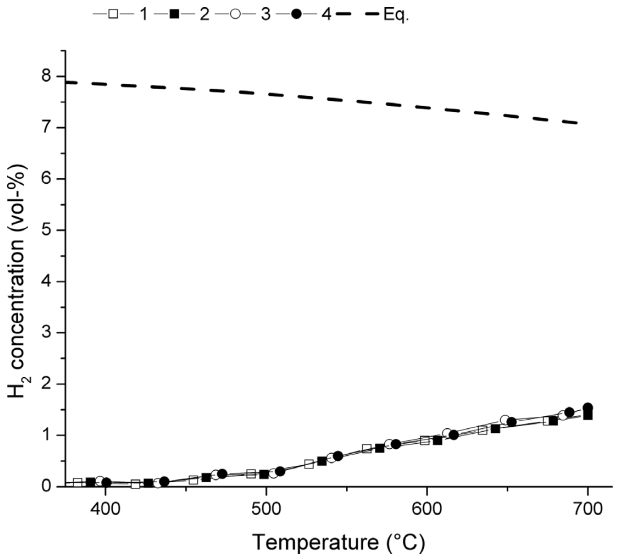

Fig. 3. H_2 concentration in the empty LF at 400–700°C.

with a logger program. The last gas analysis value from the 2 min measuring time period was considered to be the most accurate and was obtained in all gas analysis measurements.

3. Results

Reactions occurring in the LF were investigated by analyzing the gas samples taken from the GSPs 1–4 which are located at 0, 5, 10 and 15 cm heights from the bottom of the packed bed, respectively. Equilibrium concentrations of H_2 and CO gases were calculated by HSC Chemistry[11] and were plotted in the figures together with the experimental gas analyses. The equilibrium constant (K_p) of the WGSR was calculated with Eq. (2) and is plotted together with the experimental equilibrium constant values.

$$K_p = \frac{p_{CO_2} \times p_{H_2}}{p_{H_2O} \times p_{CO}}, \quad \text{..... (2)}$$

where p_i = partial pressure of gas i.

3.1. Empty Layer Furnace (ELF)

The first LF experiment was carried out in an empty layer furnace with the purpose of investigating if the forward water-gas shift reaction takes place in the LF with current set up. CO–H_2O–N_2 feed gas was used and the LF was heated at a rate of 3°C/min up to 700°C, where the heating was stopped. As seen in **Fig. 3**, H_2 concentration increases 1–2 vol-% at about 500°C practically in all GSPs indicating the WGSR. The gas composition converts towards the equilibrium through the WGSR which can be seen in the equilibrium constant curves of the WGSR shown in **Fig. 4**.

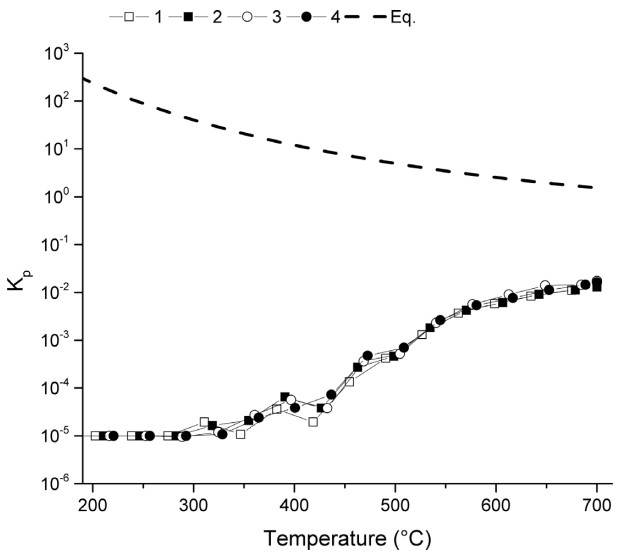

Fig. 4. Equilibrium constant of the WGSR in ELF experiment.

3.2. Hematite Pellet Layer (HPL)

Since the catalyzing effect of magnetite on the WGSR is known,[6–10] the reducing atmosphere was set to the phase stability area of magnetite (Fe_3O_4) in the $Fe_{1-y}O$–Fe_3O_4–Fe_2O_3 system with CO–CO_2–H_2O–N_2 gases for the next experiment in order to simulate the conditions in the upper BF shaft area. For the experiment the LF was filled (1.0 m layer) with hematite pellets and is labeled as HPL in Table 2. The conditions of HPL and MPL experiments are illustrated in Fe–C–H–O phase diagram shown in **Fig. 5**. The Fe–C–H–O phase diagram was drawn by the method of Oeters *et al*. 2011[13] with an assumption of 8 vol-% H_2O + H_2, 42 vol-% CO + CO_2 and 50 vol-% N_2. In HPL experiment the hematite pellets can be either reduced by CO or H_2, if the WGSR takes place. The reduction reactions of hematite to magnetite in CO and H_2 are shown in Eqs. (3) and (4).

$$3Fe_2O_3 + CO(g) = 2Fe_3O_4 + CO_2(g) \quad \text{..... (3)}$$

$$3Fe_2O_3 + H_2(g) = 2Fe_3O_4 + H_2O(g) \quad \text{..... (4)}$$

Since the WGSR was observed at around 500°C in the ELF experiment, the furnace was heated in the HPL experiment at a rate of 3°C/min up to 500°C and the gas flow was analyzed during the heating period, as shown in **Figs. 6**–**7**. Figure 6 shows that after reaching 450°C H_2 concentration increases indicating the WGSR in the pellet layer. H_2 increases first in GSP 4 and then in GSPs 3 and 2 reaching about 1–3 vol-% concentrations. In Fig. 7 it can be seen that after reaching 450°C CO decreases first in the GSP 4 and then in 3 and 2 for about 3–8 vol-%. Higher conversion of CO compared to the formation of H_2 indicates that the

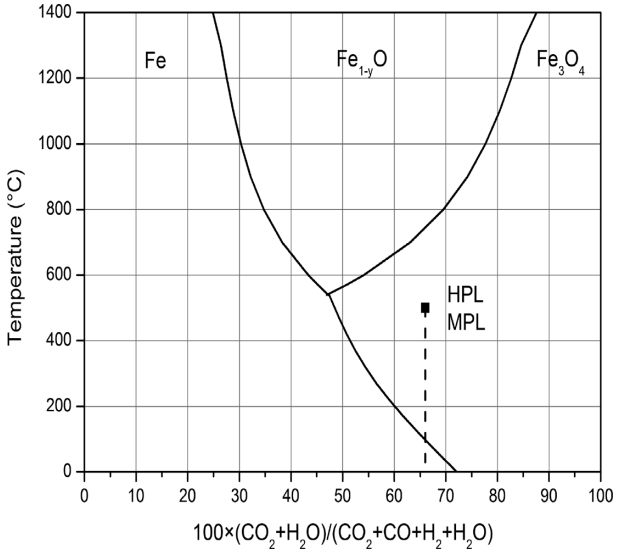

Fig. 5. Conditions of the experiments shown in Fe–C–O and Fe–H–O phase diagrams.

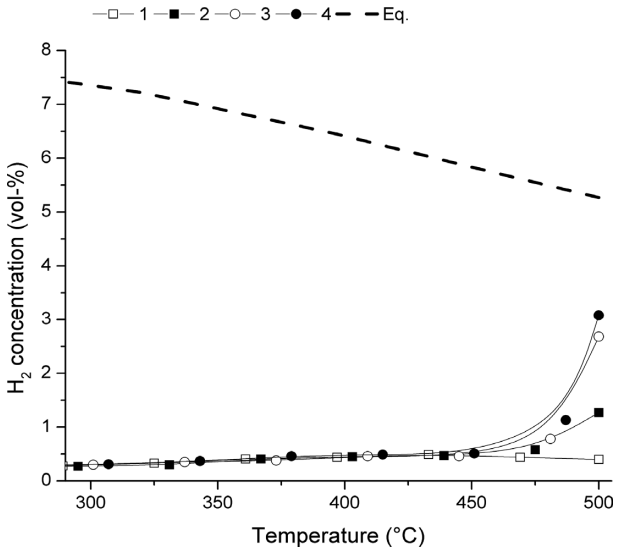

Fig. 6. H_2 concentration in the LF filled with hematite pellets at 300–500°C.

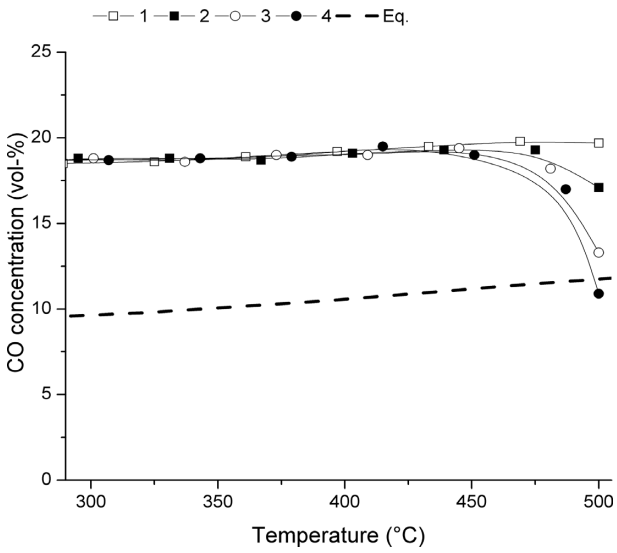

Fig. 7. CO concentration in the LF filled with hematite pellets at 300–500°C.

reduction of hematite to magnetite also takes place at these temperatures. Thus, the reduction degree and reduction rate were determined in the HPL experiment and are shown in **Figs. 8** and **9**. The reduction degree and reduction rate were calculated from the gas analyses for each 5 cm pellet layer with Eqs. (5) and (6). It should be noticed that the reduction degree and reduction rate are determined as averages for each pellet layer and the calculation method based on the gas analysis data is significantly more inaccurate compared to a weight loss method.

$$Reduction\ degree\ (\%) = \frac{\Delta m_O}{m_{O,tot}} \times 100\% \quad \text{..... (5)}$$

$$Reduction\ rate\ (mmol/s) = \frac{\Delta n_O}{\Delta t}, \quad \text{..... (6)}$$

where

Δm_o = Cumulative weight of oxygen removed from iron oxides (g)

$m_{o,tot}$ = Total weight of oxygen in iron oxides (g)

Δn_o = Amount of oxygen removed from a 5 cm pellet layer (mmol)

Δt = 120 s, time of one gas sampling period

Figure 8 indicates the pellet layers of 0–5, 5–10 and 10–

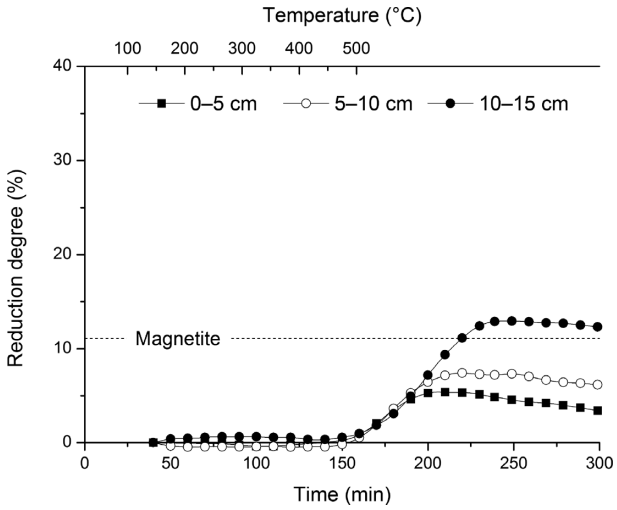

Fig. 8. Reduction degree of hematite pellets in HPL experiment.

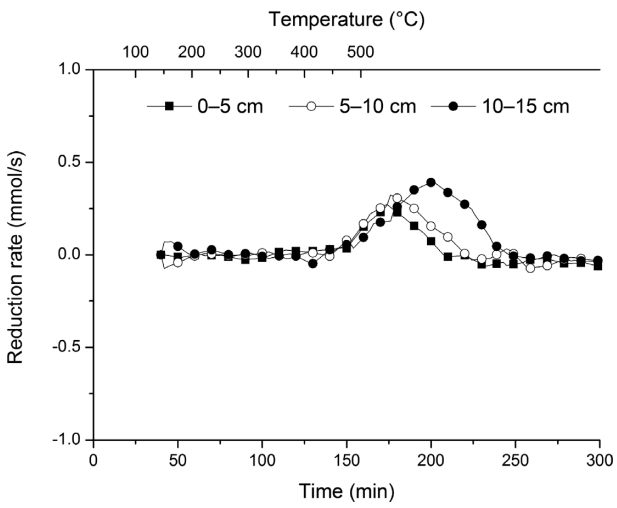

Fig. 9. Reduction rate of hematite in HPL experiment.

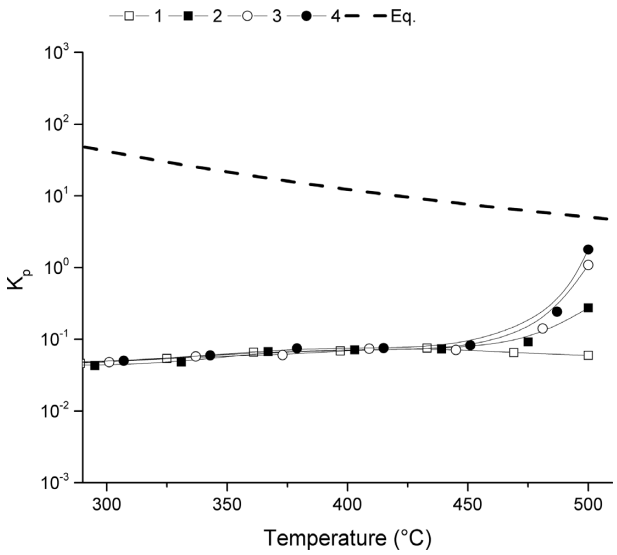

Fig. 10. Equilibrium constant of the WGSR in HPL experiment at 300–500°C.

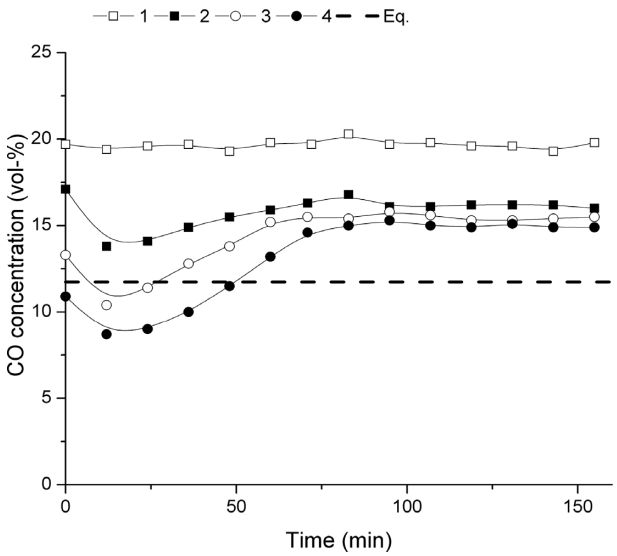

Fig. 12. CO concentration in the LF filled with hematite pellets at 500°C.

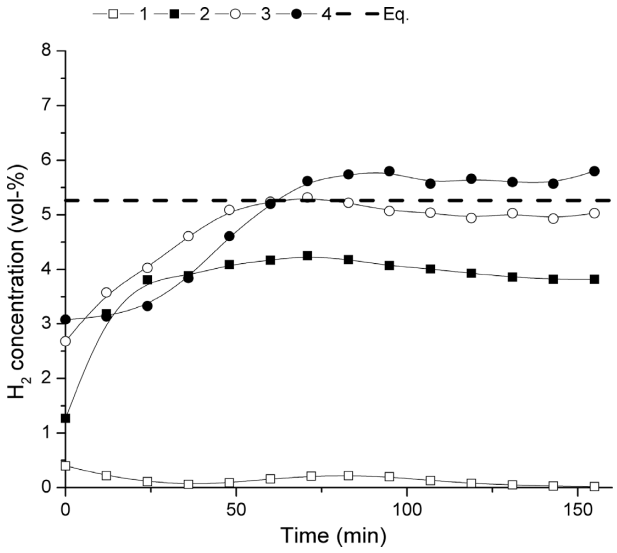

Fig. 11. H_2 concentration in the LF filled with hematite pellets at 500°C.

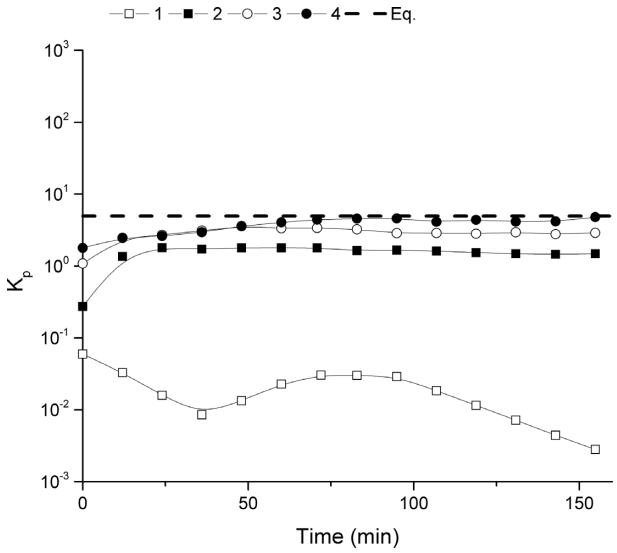

Fig. 13. Equilibrium constant of the WGSR in HPL experiment at 500°C.

15 cm have reached the hematite to magnetite reduction degree after about 200, 220 and 240 minutes, respectively. The same observation can be made in the reduction rate curves shown in Fig. 9. According to Figs. 8 and 9 the reduction degree and reduction rate are highest in the pellet layer at 10–15 cm height. The equilibrium constant of the WGSR at 300–500°C show that experimental gas converts towards equilibrium as it can be seen in **Fig. 10**. It should be noticed that experimental gas composition is here affected by the reduction and the WGSR.

After reaching 500°C, the temperature was held constant for 150 min in order to investigate the gas conversion towards the theoretical equilibrium composition at 500°C. H_2 and CO concentrations, shown in **Figs. 11** and **12**, seem to reach a steady state after 75 min in each GSP, indicating the end of the hematite to magnetite reduction. During the period between 75 and 150 min 4–6 vol-% H_2 is formed and CO concentration decreases correspondingly 4–6 vol-%. Thus, CO conversion between 75–150 min can be considered to be caused solely by the WGSR. **Figure 13** shows that the gas composition reaches theoretical equilibrium at 500°C after the hematite to magnetite reduction in the GSP 4 and almost in the GSPs 3 and 2.

3.3. Magnetite Pellet Layer (MPL)

The catalyzing effect of magnetite on the WGSR was investigated further with an experiment where olivine pellets pre-reduced to magnetite were used. The pellets were pre-reduced in the LF in the following conditions: $CO/CO_2 = 40/60$, temperature of 600°C, duration of 300 minutes and gas flow rate of 15 l/min. After reduction the pellets were cooled under a N_2 flow of 15 l/min. The feed gas and the temperature profile in the MPL experiment were identical to the HPL experiment. An increase of H_2 concentration shown in **Fig. 14** and decrease of CO shown in **Fig. 15** indicate the WGSR at the temperature range from 300 to 400°C. At first the H_2 increases in the GSP 4 at above 300°C. In the lower GSPs the WGSR is observed at slightly higher temperatures. According to **Fig. 16** the gas converts towards the equilibrium

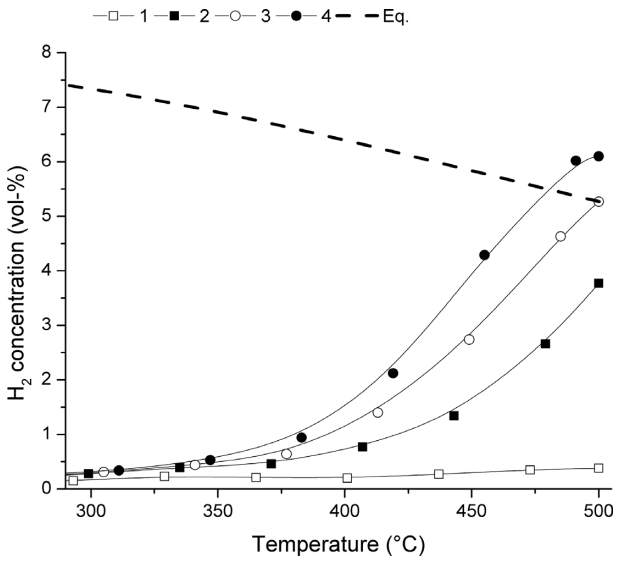

Fig. 14. H_2 concentration in the LF filled with magnetite pellets at 300–500°C.

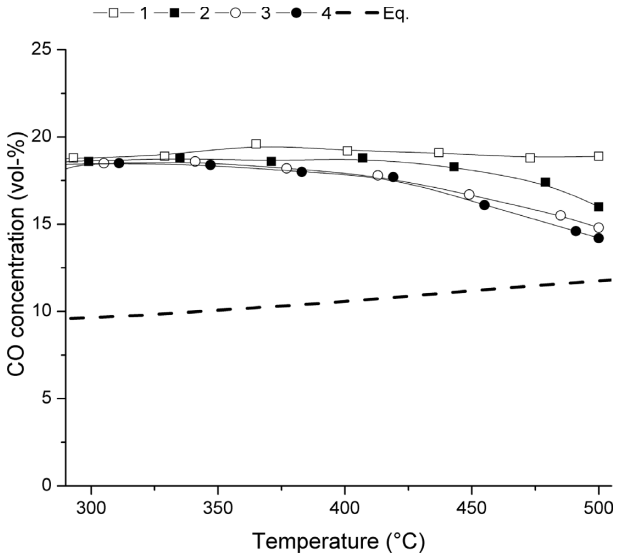

Fig. 15. CO concentration in the LF filled with magnetite pellets at 300–500°C.

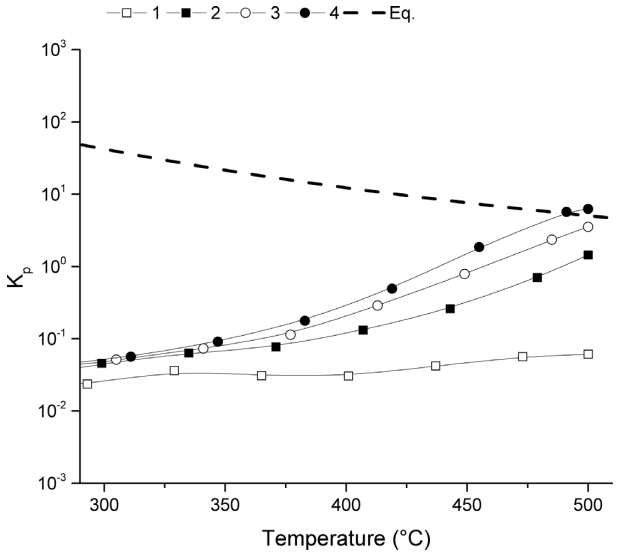

Fig. 16. Equilibrium constant of the WGSR in MPL experiment at 300–500°C.

at 300–500°C. The catalyzing effect of magnetite can be seen when these observations are compared to the results of ELF and HPL experiments. During the time LF was held at 500°C, H_2 and CO concentrations showed constant values, which can be seen in **Figs. 17** and **18**. This indicates the occurrence of the WGSR and the H_2 concentration is near to the thermodynamic equilibrium composition at 500°C in GSPs 3 and 4.

The gas converts to the equilibrium composition rapidly in the magnetite pellet layer at 500°C as shown in **Fig. 19**. Reduction reactions of iron oxides were not detected in the experiment.

3.4. Reaction Rate of the WGSR

The reaction rate of the WGSR was estimated by calculating the formation rate of H_2 in the HPL and MPL experiments. It must be noticed that the formation rate of H_2 is affected by both the reduction and the WGSR, in opposite directions. Further, the H_2 formation rate depicts the reaction rate of the WGSR when no reduction of iron oxides occurs. The formation rate of H_2 was calculated from the gas

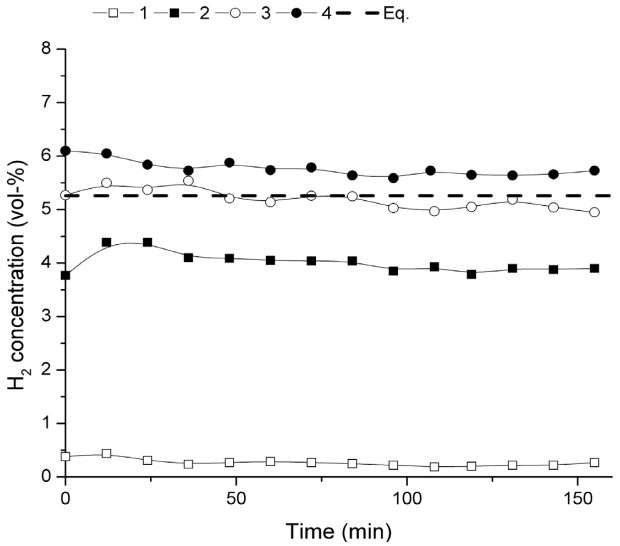

Fig. 17. H_2 concentration in the LF filled with magnetite pellets at 500°C.

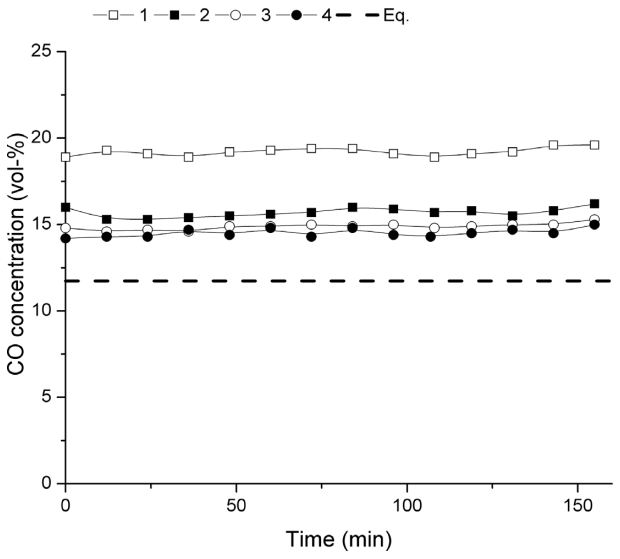

Fig. 18. CO concentration in the LF filled with magnetite pellets at 500°C.

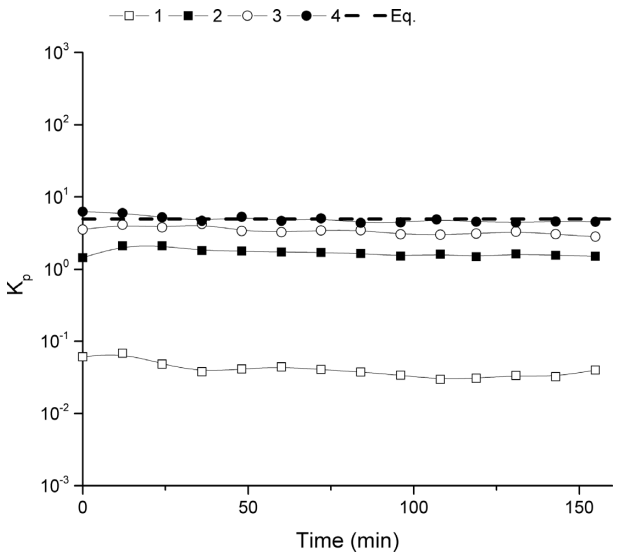

Fig. 19. Equilibrium constant of the WGSR in MPL experiment at 500°C.

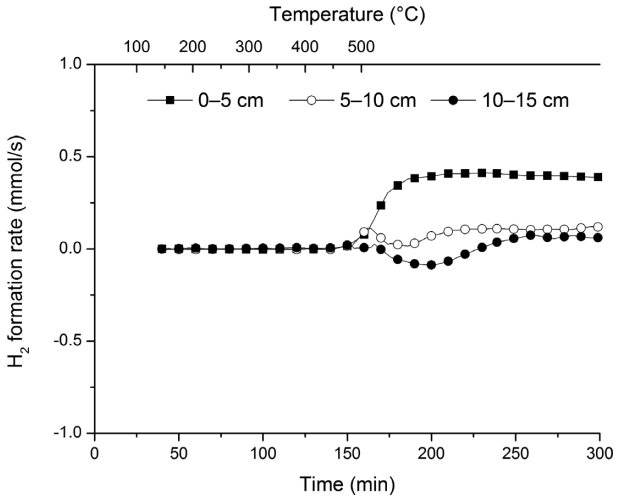

Fig. 20. Reaction rate of the WGSR in HPL experiment.

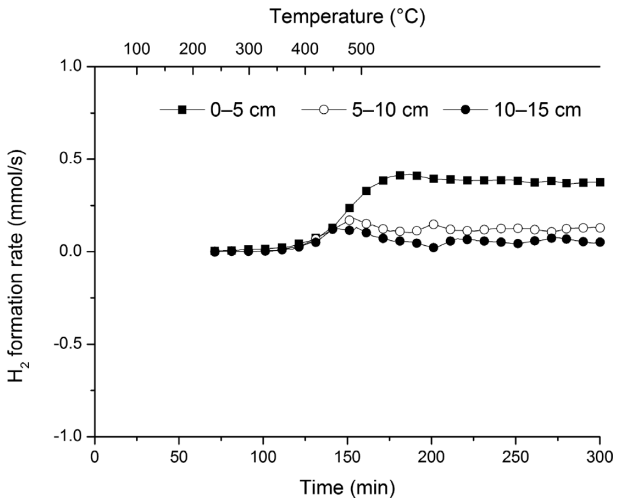

Fig. 21. Reaction rate of the WGSR in MPL experiment.

analysis data with Eq. (7).

$$\text{Formation rate}_{H_2} = \frac{\Delta H_2(\%)}{100\%} \times \frac{n}{\Delta t}, \quad \ldots\ldots\ldots\ldots (7)$$

where

$\Delta H_2(\%)$ = the change in the H_2 concentration between gas sampling points

n = amount of feed gas (mmol)

Δt = 120 s, time of one gas sampling period

The formation rates of H_2 in the HPL and MPL experiments are shown in **Figs. 20** and **21**. It was seen in the HPL experiment that the reduction of hematite ends after about 240 min and Fig. 20 shows constant formation rates of H_2 after that as well. The formation rates of H_2 in the MPL experiment show steady values after 200 min which can be seen in Fig. 21. In Figs. 20 and 21 it can be seen that the formation rate of H_2 is the highest in the lowest 5 cm part of the pellet layer and shows lower values in the higher layers. This suggests that the gas converts rapidly towards the equilibrium in the lowest 5 cm part of the pellet layer. It should be noted that no reduction reactions occurred in the MPL experiment, and therefore the H_2 formation rate illustrates solely the rate of the WGSR.

4. Discussion

4.1. The WGSR and BF Shaft Conditions

The WGSR is normally conducted in hydrogen production processes in multiple adiabatic stages with inter-stage cooling to obtain higher conversions overall, *i.e.*, high temperature shift (HTS) is conducted in the first stage where operation temperatures range from 350°C to 600°C. For HTS operation, the catalyst is typically magnetite (Fe_3O_4), the stable iron oxide phase under reaction conditions, combined with chromium oxide, which minimizes catalyst sintering. The magnetite used in HTS as the catalyst is produced by reducing hematite.[6–10] The hematite-magnetite reduction step is a sub-process in the conversion of hematite to metallic iron (Fe_2O_3–Fe_3O_4–FeO–Fe) in the BF process. According to the general understanding of the temperature and CO–CO_2 gas composition profile in the BF shaft, the conditions lead to hematite to magnetite reduction reactions in the upper BF shaft area.[14–16] Theoretically, the presence of the catalyst and a favorable temperature in the upper BF shaft area enable the progression of the forward WGSR. Although the gas approaches the equilibrium composition in the BF shaft through the WGSR, it is generally known that the BF top gas is not at thermodynamic equilibrium at the existing temperature when it exits the BF top. A typical BF top gas composition is in thermodynamic equilibrium at 600–800°C temperature.[2]

4.2. Observations from the Experiments

Slight formation of H_2 was observed in the empty layer furnace experiment (ELF) at temperatures above 500°C. In the LF experiment with hematite pellets (HPL), the WGSR was observed simultaneously with the hematite to magnetite reduction at 400–450°C. The LF experiment with pre-reduced magnetite pellets (MPL) showed indications of the WGSR at 300–400°C, showing the catalyzing effect of magnetite. Comparison of the equilibrium constants (K_p) in ELF, HPL and MPL experiments shows the gas conversion to the equilibrium at lower temperatures in the pellet layer than in the empty LF. The K_p results of the MPL experiment show the significant effect of the magnetite catalyst on the gas conversion.

After the reduction of hematite to magnetite is complete, the H_2 formation rate settles on a steady level at 500°C in the HPL experiment. In the MPL experiment, the gas conversion rate settles on the same level at the same temperature. The highest WGSR reaction rates were detected in the lowest 5 cm layer of pellets in both HPL and MPL experiments. The rate of the WGSR dropped to practically zero in the 10–15 cm part of the pellet layer. This observation indicates that the gas converts almost totally to the thermodynamic equilibrium after flowing through the lowest 10 cm layer of magnetite pellets.

4.3. Industrial Observations

At Ruukki, Raahe steelworks the BF charging procedure of iron oxides has been recently changed from mixed sinter and pellet charging to a 100% pellet charging. The charged pellets are water-treated to prevent dust emissions in addition to partial outdoor storage conditions therefore containing moisture of variable amount. At the time of mixed sinter and pellet charging the burden moisture content was in a negligible level, because the pellets were stored indoors and sinters were provided by a sinter plant situated at the steelworks. Ruukki's blast furnaces are typical modern BFs with center coke charging, where a strong gas current blows in the middle of the shaft. With the current BF charging procedure there has been detected notable change in the temperature profile of the upper part of the BF shaft. Near the charging level, the temperature is markedly lower near the walls of the shaft (50°C) with moist burden compared to the dry burden (120–130°C). In the center area of the shaft the temperature has remained approximately the same (250–400°C). Similar effect of moist burden on the temperature profile of the BF shaft has been also reported in literature.[17] These observations indicate that it is possible that moist burden descends deeper in the shaft near the BF walls, than in the middle part, before all moisture evaporates due to lower temperature and weaker gas current. The laboratory experiments of this paper showed that a gas mixture converts rapidly when a gas mixture with high water vapor concentration flows through a magnetite layer. Thus, the moisture of the burden can have effect on the BF gas composition if it evaporates in the lower parts of the shaft and the water vapor flows through a magnetite layer at a temperature above 300°C. Since the gas flow is stronger and the temperature is higher in the middle of the shaft than near the walls, it is possible that water evaporated near the walls gets swept away by the gas to the middle area of the shaft. Consequently, this can lead to the occurrence of the forward WGSR in a magnetite pellet layer. Another phenomenon, that can be considered possible, is that near the BF shaft walls the ascending water vapor condenses in the porous pellets at low temperature and descends deeper in the shaft in them until the temperature is high enough to evaporate the moisture again. This can cause water circulation in the upper BF shaft area. Evaporation of moisture and condensation of water vapor are complex processes and the determination of the critical temperatures for these phenomena to occur in a moist gas flow needs further investigation. Computational modeling can be used for these determinations and is planned for future research work. The suggested hypothesis for the burden moisture behavior near the wall in the upper part of the BF shaft and for the WGSR occurrence in the magnetite pellet layer is illustrated in **Fig. 22**.

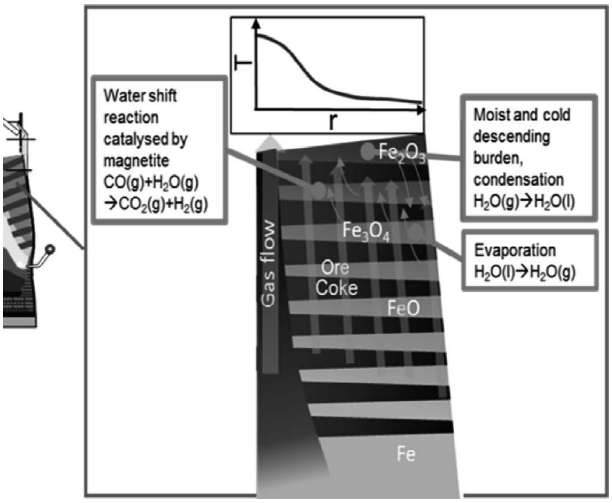

Fig. 22. Illustration of the suggested hypothesis for the burden moisture behavior near the wall in the upper part of the BF shaft and for the WGSR occurrence in the magnetite pellet layer.

4.4. Considerations about the Effects of the WGSR in the BF Shaft

According to the results of this study, it is possible that the WGSR also takes place in the BF shaft when the water vapor concentration is high and magnetite is present. This situation can occur in the BF, when ascending gas contacts a magnetite layer in the upper shaft area. The more magnetite present in the range of 300 to 600°C, the stronger the effect of the forward WGSR on the gas composition in the BF shaft can be considered to have. In literature, similar gas conversion transitioning towards equilibrium has been reported in experiments conducted on the reverse WGSR with $CO–CO_2–H_2–H_2O–N_2$ gas at high temperatures in a packed bed.[18] Studies of dissected blast furnaces have shown that the distribution of the reduction degree varies between blast furnaces and is dependent on the operating conditions.[19,20] High water vapor concentration in the upper BF shaft area can have an effect on the reduction reactions and the utilization of the BF gas, since the H_2 and CO_2 concentrations increase and H_2O and CO concentrations decrease through the WGSR, respectively. A study made by Nogami *et al*. (2012) on sinter reduction showed that a small addition of H_2 in the reducing gas increases the reduction rate of hematite but a further H_2 increase starts to decrease the reduction rate at 500°C. Higher than 2 vol-% H_2 content in the $CO–CO_2–H_2–H_2O–N_2$ gas seems not to increase the reduction rate but has a disadvantageous effect on the reduction rate, and the reduction degree obtained with 12 vol-% H_2 is the same as with 0 vol-% H_2.[5] However, when more H_2 is present in the reducing gas, the reduction-disintegration of the ore decreases improving the permeability of the burden, which need to be taken in consideration. The gas conversion caused by the WGSR changes the heat value of the BF top gas, which is usually utilized in the pre-heating process of cowper furnaces. From the viewpoint of the BF gas, the heat value of CO ($CO + 1/2O_2 = CO_2$, $\Delta H = –283.6$ kJ/mol at 200°C) is higher compared to the one of H_2 (H_2 +

$1/2O_2 = H_2O$, $\Delta H = -243.5$ kJ/mol at 200°C) which makes the occurrence of the WGSR unfavorable.[11] Also other reactions, such as the water gas reaction ($C + H_2O \rightarrow CO + H_2$), can be expected to become more significant at high temperatures (>1 000°C), lower in the BF shaft, when H_2 and H_2O concentrations are high. Since the reduction of iron oxide by H_2 is an endothermic reaction, this changes the temperature profile in the BF remarkably, which also should be considered. The effect of high H_2 and H_2O concentrations still requires further investigation in different parts of the BF shaft to obtain a better understanding of the phenomena occurring in the BF process.

5. Conclusions

In this study, the effect of the high water vapor concentration on the composition of the reducing gas through the water-gas shift reaction in the upper BF shaft area was investigated by experimental methods. The results of the layer furnace experiments can be summarized as follows:

(1) The forward WGSR was detected in the temperature range reported in literature.

(2) The WGSR was observed in the hematite pellet layer simultaneously with the hematite to magnetite reduction step at 400–450°C, indicating the catalyzing effect of the magnetite formed in the reduction reaction.

(3) In the pre-reduced magnetite pellet layer the WGSR was observed at above 300°C and the gas converted rapidly to the thermodynamic equilibrium through the WGSR. Equilibrium gas composition was reached after 15 cm layer of pellets in the LF.

(4) With high water vapor concentration the WGSR can alter the reducing gas composition in the BF shaft, when the ascending gas confronts a magnetite layer, and thus affects the reduction reactions and the utilization of the BF top gas. From the perspective of the BF gas utilization, the occurrence of the WGSR is unfavorable when the heat values of CO and H_2 are compared.

Acknowledgements

This research is a part of the Energy Efficiency & Lifecycle Efficient Metal Processes (ELEMET) research program coordinated by the Finnish Metals and Engineering Competence Cluster (FIMECC). Ruukki Metals Oy and the Finnish Funding Agency for Technology and Innovation (TEKES) are acknowledged for funding this work. Mr. Tommi Kokkonen with the University of Oulu is acknowledged for his technical support.

REFERENCES

1) A. Kemppainen, O. Mattila, E. Heikkinen, T. Paananen and T. Fabritius: *ISIJ Int*., **11** (2012), 1973.
2) T. Murakami, Y. Kamiya, T. Kodaira and E. Kasai: *ISIJ Int*., **52** (2012), 1447.
3) A. A. El-Geassy: *J. Mater. Sci.*, **21** (1986), 3889.
4) T. Usui, H. Kawabata, H. Ono-Nakazata and A. Kurosaka: *ISIJ Int*., **42** (2002), S14.
5) H. Nogami, Y. Kashiwaya and D. Yamada: *ISIJ Int*., **52** (2012), 1523.
6) D. S. Newsome: *Cat. Rev. Sci. Eng*., **21** (1980), 275.
7) C. N. Satterfield: Heterogeneous Catalysis in Industrial Practice, 2nd ed., McGraw-Hill, New York, (1991), 572.
8) C. Rhodes, G. J. Hutchings and A. M. Ward: *Catal. Today*, **23** (1995), 43.
9) C. Martos, J. Dufour and A. Ruiz: *Int. J. Hydrogen Energ*., **34** (2009), 4475.
10) B. Smith, M. Loganathany and M. S. Shantha: *Int. J. Chem. React. Eng.*, **8** (2010), R4.
11) A. Roine: Outotec HSC Chemistry ver. 7.00 for Windows, Outotec Research Oy, Pori, Finland, (2009).
12) T. Alatarvas, M. Iljana, O. Mattila, T. Paananen and T. Fabritius: Scanmet IV, 4th Int. Conf. on Process Development in Iron and Steelmaking, Vol. 1, MEFOS, Luleå, (2012), 385.
13) F. Oeters, M. Ottow, D. Senk, A. Beyzavi, J. Güntner, H. B. Lüngen, M. Koltermann and A. Buhr: Ullman's Encyclopedia of Industrial Chemistry, Vol.19, ed. by B. Elvers, John Wiley and Sons, Inc., Weinheim, (2011), 577.
14) E. Beppler, M. Kannappel, W. Kowalski, K. Langner, K. Müllheims and H. Wachsmuth: ECSC workshop, ECSC, Düsseldorf, (1998), 111.
15) A. Kasai and Y. Matsui: *ISIJ Int.*, **44** (2004), 2073.
16) K.-H. Peters, E. Beppler, B. Gerstenberg and U. Janhsen: 53rd Ironmaking Conf. Proc., Iron and Steel Society, Warrendale, PA, (1994), 257.
17) V. Ritz, K. Mülheims, R. Rosenplänter, E. Lectard and T. Bürgler: Critical review of existing procedures for the characterisation of the metallurgical properties of blast furnace burden material at conditions of high injections rates. European commission technical steel research report, Brussels, (2004), 153.
18) H. Ono-Nakazata, T. Yonezawa and T. Usui: *ISIJ Int*., **43** (2003), 1502.
19) K. Kanbara, T. Hagiwara, A. Shigemi, S. Kondo, Y. Kanayama, K. Wakabayashi and N. Hiramoro: *Trans. Iron Steel Inst. Jpn.*, **17** (1977), 372.
20) Y. Shimomura, K. Nishikawa, S. Arino, T. Katayama, Y. Hida and T. Isoyama: *Trans. Iron Steel Inst. Jpn.*, **17** (1977), 381.